Preprint of article published in Combustion Science and Technology, Vol. 188 No 11-12, pages 2267-2283, 2106. For final published version see http://dx.doi.org/10.1080/00102202.2016.121886

Chemical Kinetics of *n*-Hexane-air Atmospheres in the Boundary Layer of a Moving Hot Sphere

Rémy Mével[a], Urszula Niedzielska[b], Josué Melguizo-Gavilanes[a], Stephanie Coronel[a] and Joseph E. Shepherd[a]

[a]**California Institute of Technology**

[b] **Warsaw University of Technology**

Abstract

The present paper focuses on the chemical kinetics of the ignition of premixed *n*-hexane-air atmospheres by a moving hot sphere with emphasis on the role of low-temperature chemistry (T<1000 K). Experiments were performed to measure the minimum surface temperature for ignition of a propagating flame and non-reactive two-dimensional simulations were performed to estimate the temperature a parcel of fluid experiences as it travels within the thermal boundary layer near the surface of the sphere. Reactive simulations using detailed reaction models and a one-step model were used to investigate the chemical reaction dynamics in a constant pressure reactor with a variable heat transfer coefficient which reproduces the temperature history. It was found that, under the specific conditions studied, the chemistry is activated at T>1000 K with no noticeable impact of the low-temperature chemical pathways.

Keywords

Hydrocarbon ignition; Aircraft safety; Moving hot surface.

Short title

Ignition of n-Hexane by a Moving Hot Sphere

Introduction

The risk of accidental ignition of flammable mixtures by a hot surface is of particular importance for industrial hazards. Quantifying the risk of ignition of fuels by hot surfaces, specifically by moving hot particles, is a key issue for both engineering design and safety analyses of chemical process industry, energy generation and transportation systems. While a large number of studies have been performed on the ignition of hydrocarbons by a static hot sphere, very limited data exist on ignition by hot particles. Beyer and Markus (2012) performed studies using inert particles suspended in an explosive atmosphere and heated via laser light. The combustible mixtures used by Beyer and Markus (2012) were pentane/air, propane/air, ethylene/air and hydrogen/air. Their results showed that the particle ignition temperature was weakly dependent on equivalence ratio but was highly dependent on which gaseous fuel was used. The minimum particle surface ignition temperature required for ignition was also highly dependent on the particle diameter. More recently, Roth et al. (2014) studied the ignition of hydrogen/air mixtures by submillimeter-sized particles and determined that the particle material (silicon nitride, tungsten carbide, steel, casting steel, and aluminum) had an effect on the minimum surface temperature for ignition for a fixed mixture composition. The study by Roth et al. (2014) suggests that chemically inert particles show the lowest surface temperature required for ignition when compared to the metal particles. Additional work on stationary hot particles using laser heating has been performed by Dubaniewicz et al. (2000, 2003); Dubaniewicz (2006), Bothe et al. (1999), Beyrau et al. (2013), and Homan (1981). Hot surface ignition has also been studied for a number of fuels and surface geometries by Boettcher (2012); Boettcher et al. (2012,2013); Kuchta (1965) and Kuchta et al. (1985).

Previous experiments on moving hot particle ignition include a particle heated

in a furnace and then injected into an explosive atmosphere, as well as a stationary particle placed in an explosive atmosphere and heated via laser light. The former experiment was performed by Silver (1937) using two different particle materials, quartz and platinum. Varying the particle material had minimal effect on the minimum surface ignition temperature of three different flammable mixtures: a 10% coal-gas/air mixture, 3% pentane/air mixture, and a 20% hydrogen/air mixture. For a fixed gas mixture, the results show that the size and temperature of a particle are important factors in determining whether ignition occurs. The data indicate that as particle size increases, the minimum surface temperature required for ignition decreases. The experiments performed by Silver were done with particle speeds varying from $2 - 5$ m/s; however, the effect of particle speed was not investigated systematically. A comparison of the experimental data of Beyer and Markus (2012), and Silver (1937), for a pentane/air mixture suggests that, controlling for the diameter of the particle, a moving particle will have a higher minimum ignition temperature than a stationary particle. Paterson (1939) measured a 300 K increase in minimum ignition temperature for a 2 mm diameter sphere injected into a 9% coal-gas/air mixture at 10 m/s and later at 65 m/s. In addition, Paterson (1940) performed experiments, similar to Silver (1937), in coal-gas/air, pentane/air, and hydrogen/air, at lower particle speeds of 1.2 m/s. Paterson (1940) found a lower minimum surface temperature, by 100 K, needed for ignition of a 3% pentane/air mixture when compared to Silver's results. More recently, Coronel et al. (2013) studied the ignition of n-hexane by a hot sphere moving at a constant velocity of 2.4 m/s. Experiments were performed using 4 mm diameter spheres in n-hexane-air and n-hexane-oxygen with X_{N2}=0.40. The experiments were compared with numerical simulations of the ignition process and reasonable qualitative agreement was found but the minimum surface temperature for ignition could not be quantitatively predicted.

The goal of the present study is to investigate the chemical reaction pathways

during the ignition of n-hexane-air atmospheres by a moving hot sphere. In particular, we seek to clarify the importance of the chemical processes that occur below 1000 K for fluid elements within the thermal boundary layer of the hot sphere. A recent study by Menon et al. (2015) has demonstrated the importance of chemical activity below 1000 K during the ignition of C_6 and C_7 alkanes by a stationary concentrated hot surface. Clarifying the role of low temperature chemistry is of particular importance in the perspective of performing reactive 2-D numerical simulations of the ignition of kerosene surrogates by a moving hot sphere. In order to perform such simulations with the modest computational capabilities of most research laboratories, it is needed to reduce the available detailed reaction models and eliminate unnecessary species and reaction pathways. This process is much more difficult to carry out if reduction is needed for both low and high temperature. More importantly, the 2-D simulations would become very computationally expensive in the case of requiring an additional 20 to 30 chemical species which are needed to also describe the low temperature chemical pathways, as compared to 30 to 40 species for the high temperature chemistry. To examine this issue, we have developed an approximate approach to clarify if chemical activity takes place below 1000 K as the gas is heated within the boundary layer adjacent to the moving hot sphere. As part of this study, we have also estimated the possibility that a cool flame forms and contributes to reaction process and energy release. The experimental component of the present study was the measurement of the minimum surface ignition temperature for electrically heated titanium spheres. The likelihood of ignition for a given surface temperature is determined by statistical analysis of a series of tests. These surface temperatures were used as boundary conditions for non-reactive two-dimensional simulations of the transient viscous flow to obtain the temperature conditions the mixture experiences in the thermal boundary layer flow around a moving hot sphere. The resulting temperature profiles were used to develop a constant-pressure reactor model to simulate the ignition process for gas elements on streamlines within the boundary layer.

The reaction pathways and relative importance of the low-temperature mechanisms were examined using several detailed reaction models.

Experimental study

The ignition experiments were performed in a closed, cylindrical, stainless steel combustion vessel with a volume of approximately 22 L. Two parallel flanges were used to mount windows for visualization. Above the 22 L vessel sat a cylindrical, aluminum chamber with a volume of approximately 0.1 L. The aluminum chamber was filled with an inert atmosphere (N_2) that surrounded the metal spheres that were heated to create an ignition source. The chamber had two parallel flanges that were used to mount tungsten electrodes that were actuated linearly using pneumatic actuators. To heat a sphere, the tungsten electrodes, which were connected to a 12 V Bosch battery (CCA 850 Amps), made contact with the sphere on opposite sides. High current passed through the sphere thereby heating it. The tip of each electrode was contoured to maximize contact with the sphere to ensure minimal contact resistance and uniform heating. Figure 1 illustrates the heating process for two spheres; the spheres reached temperatures of 1200 K (top) and 1300 K (bottom). Once the desired sphere temperature was reached, one of the electrodes retracted to allow the sphere to fall. The sphere exited the inert atmosphere in the chamber and entered the combustion vessel containing the flammable gas mixture. A two-color pyrometer was used to measure the sphere surface temperature during heating. The temperature recorded during an ignition event and a no ignition event was the sphere surface temperature prior to being released. Heat transfer calculations which account for convective and radiative losses indicate that the sphere cools at most by 3% during the 250 ms fall duration. The error in the temperature measurements is $\pm 5\%$ and is due to the errors in the calibration of the two-color pyrometer (2%) as well as cooling after the sphere is released (3%). The two-color pyrometer calibration is

performed against a blackbody calibration source, however the pyrometer is used for measuring the temperature of materials with varying spectral emissivity. Accounting for the variations in spectral emissivity, the true temperature measured by the two-color pyrometer is,

$$T_{\text{true}} = \left(\frac{1}{T_{\text{measured}}} - \frac{\ln\left(\epsilon_1/\epsilon_2\right)}{C_2\left(\lambda_2^{-1} - \lambda_1^{-1}\right)} \right)^{-1}, \tag{1}$$

where T_{measured} is the temperature measured by the pyrometer, C_2 is a Planck constant, ϵ_1 and ϵ_2 are the emissivities at the optical wavelengths λ_1 and λ_2, respectively. For titanium, the ratio $\epsilon_1/\epsilon_2 \approx 0.99$ from Teodorescu and Jones (2008) for $\lambda_1 = 1705nm$ and $\lambda_2 = 1940nm$.

Ignition tests were performed for n-hexane-air mixtures at an initial temperature and pressure of 298 K and 100 kPa, respectively. The mixture equivalence ratio, Φ, was fixed at 0.9 and titanium (Ti-6Al-4V) spheres 4 mm in diameter were used. Examples of schlieren images for an ignition and a no ignition case are shown in Figure 2. A series of 36 experiments was performed to obtain the ignition results shown in Figure 3. A cumulative probability distribution, indicated by the black line, was obtained through the logistic regression method described in Bane (2010). The likelihood function shown in Eq. 2,

$$L = \prod_{i=1}^{n} P\left(x_i\right)^{y_i} \left(1 - P\left(x_i\right)\right)^{1-y_i}, \tag{2}$$

where $P\left(x\right)$ is a parametric logistic distribution function,

$$P\left(x\right) = \frac{1}{1 + \exp\left(-\beta_0 - \beta_1 x\right)}, \tag{3}$$

is maximized to obtain the parameters β_0 and β_1. In Equation 2, x_i is the stimulus level or surface temperature, n is the number of trials, and y_i is the binary result, 0

for no ignition and 1 for ignition. Figure 3 shows the corresponding 95% confidence intervals in red dashed lines. The ignition results are shown by the open circles, an ignition event has a probability of ignition value of 1 and a no ignition event has a probability of ignition value of 0. A narrow overlap region of $1150 - 1175$ K exists between the ignition and no ignition results; this overlap can be attributed to uncertainty in the temperature measurements, variability in the speed of the sphere, deviations in the the sphere trajectories, and other unquantified variations in measurements of experimental conditions.

Temperature time history within the boundary layer

To obtain the temperature time histories of selected fluid elements within the boundary layer of the moving hot sphere, non-reactive two-dimensional simulations were carried out using a range of sphere temperatures consistent with the experimental results shown in Figure 3. The computations were performed using the Open source Field Operation And Manipulation (OpenFOAM) toolbox (Weller et al., 1998) to solve the Navier-Stokes equations with temperature dependent transport properties. The Sutherland Law, the Eucken Relation and the JANAF polynomials were used to account for the functional temperature dependence of mixture viscosity (μ), thermal conductivity (κ) and specific heat at constant pressure (c_p), respectively. The gas was assumed to be pure nitrogen for the purposes of estimating the thermal boundary layer.

$$\frac{\partial \rho}{\partial t} + \nabla \cdot (\rho \mathbf{u}) = 0 \tag{4}$$

$$\frac{\partial (\rho \mathbf{u})}{\partial t} + \nabla \cdot (\rho \mathbf{u}\mathbf{u}) = -\nabla P + \nabla \cdot \tau + \rho \mathbf{g} \tag{5}$$

$$\frac{\partial (\rho h_s)}{\partial t} + \nabla \cdot (\rho \mathbf{u} h_s) = \nabla \cdot (\kappa / c_p \nabla h_s) \tag{6}$$

$$\text{with } \; P = \rho \bar{R} T, \;\; h_s = c_p T, \;\; \tau = \mu[\nabla \mathbf{u} + (\nabla \mathbf{u})^T] - \frac{2}{3}\mu(\nabla \cdot \mathbf{u})\mathbf{I} \tag{7}$$

where ρ is the density, t is the time, u is the velocity vector, P is the pressure, g is the gravitational acceleration, h_s is the sensible enthalpy, T is the temperature, τ is the deviatoric stress tensor, I is the identity tensor, and $\bar{R}$ is the specific gas constant. The computational domain consisted of a vertical rectangle with a 2D-axisymmetric sphere located at (x, y, z) = (0, 0, 0) with a diameter d=4 mm. The top, bottom and side boundaries were placed $15d$, $5d$ and $10d$ away from the center of the sphere, respectively. A resolution of approximately 300,000 cells was used, refined non-uniformly near the sphere, with a minimum cell size of 60 μm to ensure that the thermal and hydrodynamic boundary layers were properly resolved. The initial conditions are the same as in the experiment, i.e. P_1=100 kPa, T_1=300 K, U_1=0 m/s and X_{N2}=1. Five cases were run with sphere surface temperatures, T_{sphere}, ranging from 1200 K to 1600 K at 100 K intervals. The frame of reference was attached to the sphere, and a time dependent inflow boundary condition was prescribed at the bottom of the computational domain to simulate the fall of the heated particle as experienced in the experiments, the drag is negligible at this stage and velocity increases at a rate of 9.81 m/s^2. At the top, a non-reflective/pressure transmissive boundary condition was used to simulate an outflow. The simulation was performed for 0.25 s, (experimental fall time before contact with reactive mixture), then, five streamlines (SL) within the thermal boundary layer were selected for analysis. The properties (temperature, velocity and position) extracted (see Figure 4 a) along the strealines; temperature histories for particles traveling on strealimes 1, 3 and 5 are shown in Figure 4 b).

Chemical reaction modeling

Reaction model performance

Several detailed reaction models that include the kinetics of n-hexane were employed to model the reaction of n-hexane-air at Φ=0.9: (i) Ramirez et al. (2011), 1789 re-

actions and 401 species, (ii) Mével et al. (2014), 2628 reactions and 531 species; (iii) Blanquart et al. (2009), 1119 reactions and 172 species; (iv) Livermore (Mehl et al., 2011), 2827 reactions and 654 species; and (v) JetSurf (Wang et al., 2010), 2163 reactions and 348 species.

The performance of the models over a range of initial conditions was examined by computing the idealized ignition delay time, shown in Figure 5 a), defined as the time to maximum temperature gradient, using the constant-pressure reactor model in Senkin (Lutz et al., 1992) of the Chemkin II package (Kee et al., 1993). The models can be divided into two groups: (i) JetSurf and Blanquart models that do not include low-temperature chemistry for n-hexane, and (ii) the Ramirez, Mével, and Livermore models which include the low-temperature chemistry for n-hexane. Without the low-temperature chemistry, non-physical ignition delay times are predicted in the range 600-800 K. At high-temperature, the predictions of the five models are similar except for the Ramirez mechanism which exhibits significantly longer delay times. In Figure 5 b), the ratios between the predicted delay times of the different models are plotted as a function of reciprocal temperature. At high temperature, the model of Mével predicts the shortest ignition delay times whereas the model of Ramirez et al. predicts the longest delay times. At temperature below 1000 K, the model of Livermore predicts much shorter ignition delay times when compared to the two other models (Mével and Ramirez) which include low temperature chemistry. The characteristic difference in induction delay time at low temperatures highlights the importance of the role of the low-temperature chemistry on the ignition process within the sphere boundary layer if there are sufficiently low temperatures and long residence times.

The validity of the reaction models was verified against shock-tube ignition delay time data, experiments of Zhukov et al. (2004); Burcat el al. (1992,1996) and

Davidson et al. (2010). In addition, we performed a number of shock-tube experiments in our laboratory using highly argon-diluted *n*-hexane-oxygen mixtures. The shock-tube employed has been described in detail in Mével et al. (2013), Chatelain et al. (2014) and Mével and Shepherd (2015). Three emission signals were monitored simultaneously; these were OH*, CH* and CO_2*. We also used for validation the ignition data from Campbell et al. (2015) that were obtained for *n*-heptane-based mixtures. Campbell's results have been used because of the lack of data for *n*-hexane at low-temperature and the similarity in terms of reactivity between the two fuels, see Davidson et al. (2010). The available experimental data on *n*-hexane ignition behind shock waves, along *n*-heptane data from Campbell et al., cover the following ranges: Φ=0.5-2; $X_{Diluent}$=0.7898-0.96; T=650-1760 K; and P=0.178-22.5 MPa. The validation study was performed for three models: Mével, Blanquart and Livermore. The JetSurf model was not considered because its predictions are very close to those of Blanquart's model. The model of Mével is an updated version of Ramirez et al. model, therefore, this older version was not further considered.

In Figure 6, the predictions of the models are compared with the data of Zhukov et al. (2004) and Burcat el al. (1992, 1996). For the highest reflected shock pressures studied by Zhukov et al., the models of Mével et al. and of Livermore are in reasonable agreement with the experimental data. At the lowest pressure used by Zhukov, the model of Livermore overestimates the measured delay time. The model of Blanquart significantly overestimates the data of Zhukov et al. with an average error of 460%. The mean error for Mével and Livermore models are 20% and 52%, respectively. For the data of Burcat et al., none of the models are able to reproduce with reasonable accuracy the measured delay time over the full temperature range. The model of Mével better matches the data obtained at low temperature whereas the model of Livermore better reproduces the data at high temperature. Blanquart's and Mével's model demonstrate a mean error around 42% whereas Liv-

ermore's model exhibits a mean error of 63%. In Figure 7, the predictions of the three models are compared to the experimental temperature resolved species profiles from Burcat et al. (1996). Mével's model gives the best quantitative agreement among the three models. The two other models under estimate the mole fraction by about an order of magnitude.

Figure 8 a) and b) show the predictions of the three models, Mével, Blanquart and Livermore, as compared with the experimental data of the present study and of Davidson et al. (2010), respectively. All the models reproduce the activation energy of the ignition process observed experimentally. The model of Livermore tends to overestimate the delay time whereas the model of Mével predicts the shortest ignition delay time. The mean errors are 17%, 21% and 65% for Mével, Blanquart and Livermore, respectively, when compared to the present study. For Davidson et al. experimental results, the mean errors are 12% for Blanquart and about 40% for Mével and Livermore. In Figure 8 c), the predictions of the models of Mével et al. and of Livermore for n-hexane-based mixtures are compared with the experimental results of Campbell et al. (2015) (obtained with n-heptane). Mével's model predicts faster ignition at high temperature, and is in very good agreement with the experimental data but does not reproduce very well the first-stage ignition in the low-temperature range in contrast to Livermore's model predictions. In the low-temperature range, the model of Mével over estimates by a factor of two the ignition delay time obtained experimentally.

Chemical reactions on streamlines

To estimate the chemical activity under conditions representative of those encountered during heating of n-hexane-air by a moving hot sphere, constant pressure simulations were performed in a closed 0-D reactor with a time-dependent heat

transfer coefficient. The reactor is described by

$$\rho c_P \frac{dT}{dt} = \sum_{i=1}^{n} \dot{\omega}_i h_i + \frac{S}{V} H(t)(T_s(t) - T) \tag{8}$$

$$\rho \frac{dY_i}{dt} = \dot{\omega}_i W_i \tag{9}$$

where n is the total number of species; V is the volume of the reactor; ρ the density; c_P the heat capacity at constant pressure; T the temperature; t the time; $\dot{\omega}_i$ the chemical production rate of the ith species; h_i the enthalpy of the ith species; S the surface of the reactor; $H(t)$ the heat transfer coefficient; Y_i the mass fraction of the ith species; and W_i the molecular weight of the ith species. During the heating period, the reactor received energy from a hot surface maintained at a fixed temperature of T$_s$=1200-1600 K. During the cooling period, the reactor loses energy to a surface whose temperature, $T_s(t)$, progressively drops to 300 K. The heat transfer coefficient $H(t)$ varies with time to reproduce the temperature profile obtained in the two-dimensional simulation for the streamline closest to the sphere surface, SL5. This streamline was located at a distance of 0.367 mm from the surface at the separation point. Maximum deviations on the order of 20 K were observed between the temperature profile obtained in the 2-D simulation and that used in the 0-D simulation during the initial (heating) and intermediate (plateau) stages; slightly larger deviations, up to 40-50 K were observed during the cooling phase. When the chemical energy release rate significantly exceeds the heat losses to the wall, the temperature profile deviates from the prescribed non-reactive history, indicating that ignition is taking place. If the energy release by the chemistry is less than or equal to the heat losses, the temperature profile simply follows the prescribed non-reactive history. Note that this model cannot accurately predict ignition thresholds but is useful to examine the role of chemistry before ignition takes place and to provide a conservative value for the surface temperature at which ignition is likely to occur. On of the main limitations of this model is that it does not account for

the diffusion of species from adjacent streamlines. Another is the use of an empirical heat transfer coefficient, $H(t)$, rather than actual thermal diffusion with the boundary layer. These are issues that we are examining in ongoing studies using the full reactive Navier-Stokes simulations with detailed and reduced reaction models. Preliminary results show that the diffusion of reactive radicals and atoms away from the zone of flow separation, where ignition is the likely to occur when close to the ignition threshold, delays ignition and thus pushes the ignition threshold towards higher temperatures. Consequently, the present simplified model yields a bounding estimate of the minimum temperature at which ignition should occur.

Figure 9 shows the evolution of the temperature along the closest streamline predicted by several reaction models for all the surface temperatures considered. The model of Mével predicts a minimum ignition temperature for T_s=1300 K whereas the models of Blanquart and Livermore do not predict ignition below 1400 K. To examine the performance of the most simplified possible reduced mechanism, a one-step reaction model was created based on matching high-temperature ignition delay times computed from Mével's detailed reaction model. This simple model is described by: Reactant→Product; chemical energy: q_{chem}=2.461×10^6 J/kg; and reaction rate: k=0.1618×$T^{2.989}$×exp(-158280/RT). As seen in Figure 9 b), the one-step model predictions are consistent with those of Mével's model with ignition occurring at T_s=1300 K. The lowest temperature for which ignition occurs in the 0-D simulations is close to 1300 K. The detailed reaction model indicates that the low-temperature chemistry does not play a significant role during the ignition of *n*-hexane for the cases we have examined. One of the main reasons for this is the short residence time, 5 to 10 ms, of the gas elements on the streamlines, see Figure 4, in comparison to the characteristic low-temperature delay times of 100's ms. The short residence time prevents the accumulation of species, such as hydroperoxides, important to the low temperature chemical reaction pathways.

Figure 10 shows the temperature and species profiles, and Figure 11 shows the most important reaction pathways. Figure 10 and Figure 11 were obtained with Mével's model at T_s=1200 and 1300 K. For the no-ignition case, T_s=1200 K, very little consumption of the reactants is observed. Formation and accumulation of C_2H_4, H_2, CO, H_2O_2, H_2O and CO_2 are observed. (Note that for clarity, H_2 and H_2O reservoirs are not displayed in the Figure 11.) As seen in Figure 11, no significant pathways are available to consume C_2H_4. A small amount of OH radical is produced but the OH concentration drops down as the temperature decreases. This is due to the low extent of the chain branching process taking place at this temperature with only 6% of oxygen consumed by H atoms. Both H and OH primarily react with *n*-hexane to form hexyl radicals and H_2 and H_2O, respectively. This indicates that pyrolysis and partial oxidation are favored in the range of temperatures that the mixture experiences for T_{sphere}=1200 K. In the ignition case, T_s=1300 K, a large fraction of the initial fuel is converted to C_2H_4 and H_2 before ignition occurs. At the same time, the concentrations of CO, CO_2 and OH increase progressively and then very rapidly as ignition occurs. Rapid formation of the OH radical is sustained by branching processes with 45% of O_2 consumed by H. The formation of CO_2 is mostly due to CO+OH=CO_2+H which sustains the regeneration of H atoms along with significant heat release. For both T_s=1200 and 1300 K cases, very little chemical activity is observed during the heating period which is too short for reactions to proceed. The mixture is rapidly heated to the peak temperature and it is the time spent at this high-temperature portion of the process that determines if ignition occurs.

The present approach constitutes a highly simplified approximation of the ignition of flammable atmospheres by a moving hot sphere. Whereas we consider all the possible chemical pathways, our simplified model does not account for the effect of

species diffusion and the thermal diffusion model is highly simplified. Simulations of the flow performed with a full detailed reaction model by Melguizo-Gavilanes et al. (2015) for hydrogen-air mixtures indicate that the process of ignition depends on the balance of thermal energy and species generation rates along the streamlines, effects which our simple model cannot reproduce. Detailed 2D reactive Navier-Stokes simulations reveal that the ignition events take place some distance away from the hot surface and quantitative prediction of ignition threshold require accurate representation of the balance of transport and reaction processes. Diffusion of species could influence the ignition process in two ways: (i) by delaying the formation of a flammable atmosphere close to the sphere surface where the temperature is high enough to trigger ignition, and (ii) by removing active radicals, especially H atom which exhibits the highest diffusivity, from the region of high temperature where their rate of production is the highest. Experimentally, the sphere has to be heated in an inert atmosphere (N_2) to prevent ignition during this phase and a N_2 boundary layer develops around the sphere during its fall prior to contact with the reactive mixture. The reactive mixture must penetrate the boundary layer and diffuse to the surface in order for ignition to take place. Under the conditions of our experiments, this takes sufficiently long that the mixture in the thermal boundary layer is highly non uniform in dilution amount and that preferential diffusion may modify the equivalence ratio as compared to the initial composition of the quiescent reactive mixture. Removal of active species through diffusion after chemical activity is activated could create a balance between their production through chemistry and their losses through transport, preventing the progress of the chemical reactions. However, this removal process is not likely to activate low temperature chemistry away from the hot sphere because, as seen in Figure 4, the residence time in these streamlines is much shorter than the chemical timescales at these lower temperatures.

Conclusion

In the present study, the role of low-temperature chemical reaction pathways for the ignition of n-hexane-air by a moving hot sphere has been analyzed. Experiments were carried out to measure the minimum sphere surface temperature at which ignition occurs. Non-reactive two-dimensional simulations were performed using these temperatures as boundary conditions to quantify the typical temperature history that a parcel of fluid experiences within the boundary layer of the hot sphere. Using these temperature histories and an empirical model of heat transfer, the chemical activity predicted by several detailed reaction mechanisms as well as a one-step model was studied. The results indicate that because of the short residence time of most fluid elements within the boundary layer under the conditions considered, the low-temperature chemistry does not play a significant role in the ignition process. This conclusion cannot be reached by simply comparing the residence time of the gas in the thermal boundary layer to the ignition delay time. The time to ignition is not the right time scale to take into account to estimate the importance of low-temperature chemical process. The temperature-time history is important to consider when evaluating the relevance of low-temperature reaction processes. Results of Campbell et al. (2015) demonstrate that significant chemical activity can be initiated during the so-called first stage ignition within a time scale much shorter than the time to ignition as defined by a strong temperature increase. This aspect has also been studied by Zhao et al. (2016) who showed that a cool flame can be initiated by a pocket of gas at relatively low-temperature and lead to the formation of a regular hot flame. Under the conditions of the present study, such phenomena were not observed due to the specific temperature histories used to model the heating process in the boundary layer. The results are encouraging for using simplified models but further study is needed to examine the role of realistic species and thermal diffusion in the chemical reaction processes at low temperatures. Other geometries and slower heating rates

may lead to longer residence times at low temperature that results in greater role for low-temperature reaction mechanisms.

Acknowledgments

The present work was performed at the Explosion Dynamics Laboratory of the California Institute of Technology and was partly supported by The Boeing Company through a Strategic Research and Development Relationship Agreement CT-BA-GTA-1 with Arthur Day as a technical monitor. Urszula Niedzielska is grateful to Polish-U.S. Fulbright Commission for sponsoring her stay at Caltech as a Visiting Special Student. Josué Melguizo-Gavilanes is grateful to the Natural Sciences and Engineering Research Council of Canada (NSERC) for providing a Postdoctoral Fellowship.

References

Bane S. (2010) Spark ignition: experimental and numerical investigation with application to aviation safety. PhD thesis: California Institute of Technology.

Beyer M. and Markus, D. (2012). Ignition of explosive atmospheres by small hot particles : Comparison of experiments and simulations. Sci. Technol. Energ. Ma., 73, 1.

Beyrau F., Hadjipanayis M. A., and Lindstedt R. P. (2103) Ignition of fuel/air mixtures by radiatively heated particles. Proc. Combust. Instit., 34, 2065-2072

Blanquart G., Pepiot-Desjardins P., and Pitsch H. (2009) Chemical mechanism for high temperature combustion of engine relevant fuels with emphasis on soot precursors. Comb. Flame, 156, 588.

Boettcher P.A., Mével R., Thomas V. and Shepherd J.E. (2012) The effect of heating rates on low temperature hexane air combustion. Fuel, 96, 392.

Boettcher P.A. (2012) Thermal Ignition. PhD thesis: California Institute of Technology.

Boettcher P., Menon S., Ventura B., Blanquart G. and Shepherd J. (2013) Cyclic flame propagation in premixed combustion. J. Fluid Mech., 735, 176.

Bothe H., Schenk S., Hawksworth S., Carleton F., and Weinberg F. (1999) The safe use of optics in potentially explosive atmospheres. Explosion Safety in Hazardous Areas (Conf. Publ. No. 469), 44.

Burcat A., Pitz W.J. and Westbrook C.K. (1992) Comparative ignition of hexane and octane isomers in a shock-tube. International Symposium on Shock Waves, 18, 771.

Burcat A., Olchanski E. and Sokolinski C. (1996) Kinetics of hexane combustion in a shock tube. Isr. J. Chem., 36, 313.

Campbell M.F., Wang S., Goldenstein C., Spearrin R. M., Tulgestke A., Zaczek L., Davidson D., and Hanson R. (2015) Constrained reaction volume shock tube study of n-heptane oxidation: Ignition delay times and time-histories of multiple species and temperature. Proc. Combust. Instit., 35, 231.

Chatelain K., Mével R., Menon S., Blanquart G. and Shepherd J. (2014) Ignition and chemical kinetics of acrolein-oxygen-argon mixtures behind reflected shock waves. Fuel, 135, 498.

Coronel S.A., Menon S., Mével R., Blanquart G. and Shepherd J.E. (2013) Ignition of nitrogen diluted hexane-oxygen mixtures by moving heated particles. Proceedings of the ICDERS 24: paper 239.

Davidson D.F., Ranganath S.C., Lam K.-Y., Liaw M., Hong Z. and Hanson R.K. (2010) Ignition Delay Time Measurements of Normal Alkanes and Simple Oxygenates. J. Propul. Power, 26, 280.

Dubaniewicz T. H., Cashdollar K. L., Green G. M., and Chaiken R. F. (2000) Ignition of methane-air mixtures by laser heated small particles. J. Loss Prevent. Proc., 13, 349.

Dubaniewicz T. H., Cashdollar K. L., and Green G. M. (2003) Continuous wave laser ignition thresholds of coal dust clouds. J. Laser Appl., 15, 184.

Dubaniewicz T. H. (2006) Threshold powers and delays for igniting propane and butane-air mixtures by cw laser-heated small particles. J. Laser Appl., 18, 312.

Homan H. S. (1981) Minimum Mass of Burning Aluminum Particles for Ignition of Methane/Air and Propane/Air Mixtures. Symp. (Int.) Combust., 18, 1709.

Kee R., Rupley F. and Miller J. (1993) CHEMKIN II: A Fortran chemical kinetics package for the analysis of gas phase chemical kinetics. Technical report: Sandia International Laboratories.

Kuchta J.M. (1985) Investigation of Fire and Explosion Accidents in the Chemical, Mining, and Fuel-Related Industries. Technical report: Bureau of Mines.

Kuchta J.M., Bartkowiak A. and Zabetakis M.G. (1965) Hot Surface Ignition Temperatures of Hydrocarbon Fuel Vapor-Air Mixtures. J. Chem. Eng. Data, 10, 282.

Lutz A., Kee R. and Miller J. (1992) SENKIN: a fortran program for predicting homogeneous gas phase chemical kinetics with sensitivity analysis. Technical report: Sandia International Laboratories.

Mehl M., Pitz W.J., Westbrook C.K., Yasunaga K., Conroy C. and Curran H.J. (2011) Autoignition behavior of unsaturated hydrocarbons in the low and high temperature regions. Proc. Combust. Instit., 33, 201.

Melguizo-Gavilanez J., Coronel, S., Mével, R., and Shepherd, J.E. (2015) Ignition of hydrogen-air mixtures by moving heated particles. Proceedings of the 6^{th} International Conference on Hydrogen Safety.

Menon S., Boettcher P., Ventura B. and Blanquart G. (2015) Hot surface ignition of C_6 and C_7 hydrocarbons in air. Comb. Flame. in press.

Mével R., Pichon S., Catoire L., Chaumeix N., Paillard C.E. and Shepherd J.E. (2013) Dynamics of excited hydroxyl radicals in hydrogen-based mixtures behind reflected shock waves. Proc. Combust. Instit., 34, 677.

Mével r., Chatelain K., Boettcher P.A. and Shepherd J.E. (2014) Low temperature oxidation of n-hexane in a flow reactor. Fuel, 126, 282.

Mével R. and Shepherd J.E. (2015) Ignition delay-time behind reflected shock waves of small hydrocarbons-nitrous oxide(-oxygen) mixtures Shock Waves, 25, 217.

Paterson S. (1939) I. The ignition of inflammable gases by hot moving particles. The London, Edinburgh, and Dublin Phil. Mag. and J. of Science, 28, 1-23

Paterson S. (1940) XLII. The ignition of inflammable gases by hot moving particles. The London, Edinburgh, and Dublin Phil. Mag. and J. of Science, 30, 437-457

Ramirez H., Hadj-Ali K., Dievart P., Dayma G., Togbe C., Moreac G., and Dagaut P. (2011) Oxidation of commercial and surrogate bio-diesel fuels (B30) in a jet-stirred reactor at elevated pressure: Experimental and modeling kinetic

study. Proc. Combust. Instit., 33, 375.

Roth D., Sharma P., Haeber T., Schiessl R., Bockhorn H., and Maas U. (2014) Ignition by Mechanical Sparks: Ignition of Hydrogen/Air Mixtures by Submillimeter-Sized Hot Particles. Combust. Sci. Technol., 186, 1606-1617

Silver R.S. (1937). The ignition of gaseous mixtures by hot particles. The London, Edinburgh, and Dublin Phil. Mag. and J. of Science, 23:156, Suppl. April 1937, pp. 633-657

Teodorescu G. and Jones P.D. (2008). Spectral and directional emittance of alumina at 823 K. J. Mater. Sci., 43, 7225-7229

Wang H., Dames E., Sirjean B., Sheen D., Tangko R., Violi A., Lai J., Egolfopoulos F., Davidson D., Hanson R., Bowman C., Law C., Tsang W., Cernansky N., Miller D.L. and Lindstedt R. (2010) A high-temperature chemical kinetic model of n-alkane (up to n-dodecane), cyclohexane, and methyl-, ethyl-, n-propyl and n-butyl-cyclohexane oxidation at high temperatures, JetSurF version 2.0.

Weller H.G., Tabor G., Jasak H. and Fureby C. (1998). A tensorial approach to computational continuum mechanics using object-oriented techniques. Comput. Phys., 12, 620.

Zhao P., Liang, W., Deng S. and Law C. (2016) Initiation and propagation of laminar premixed cool flames Fuel, 166, 477

Zhukov V., Sechenov V. and Starikovskii A.Y. (2004) Ignition delay times in lean n-hexane-air mixture at high pressures Comb. Flame, 136, 257.

Figure captions

Figures

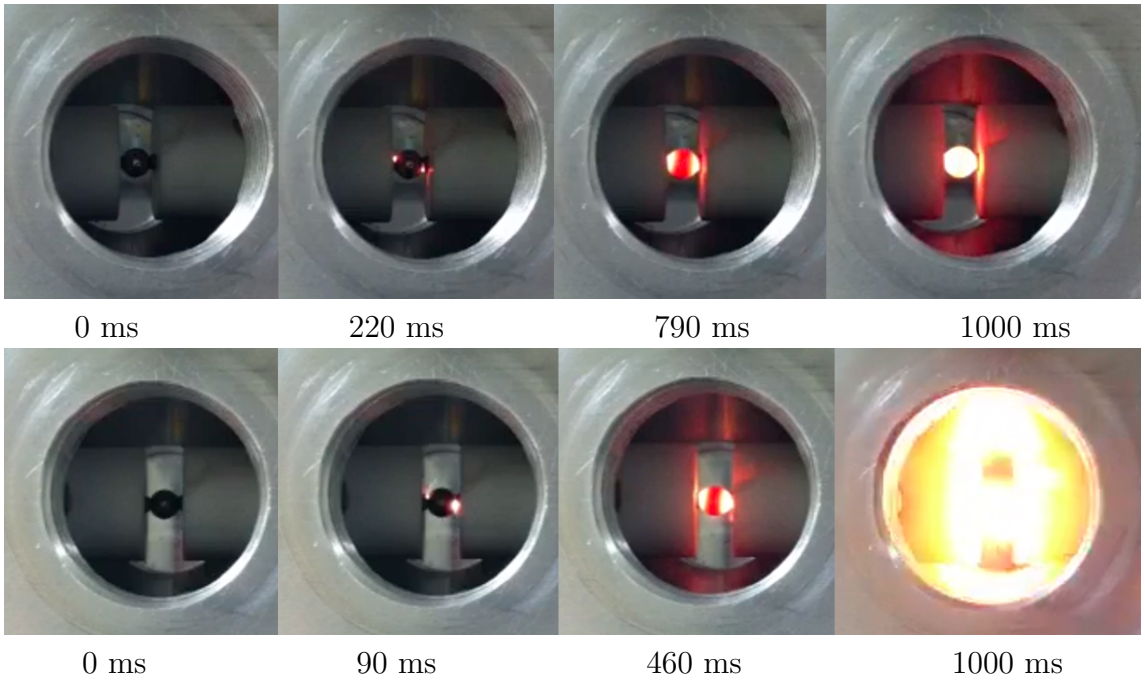

Figure 1: Sequence of images of the heating of a 4 mm titanium sphere by electrical current. Conditions: heating time$\simeq$ 1 s Top: T_{sphere}=1200 K; Bottom: T_{sphere}=1300 K.

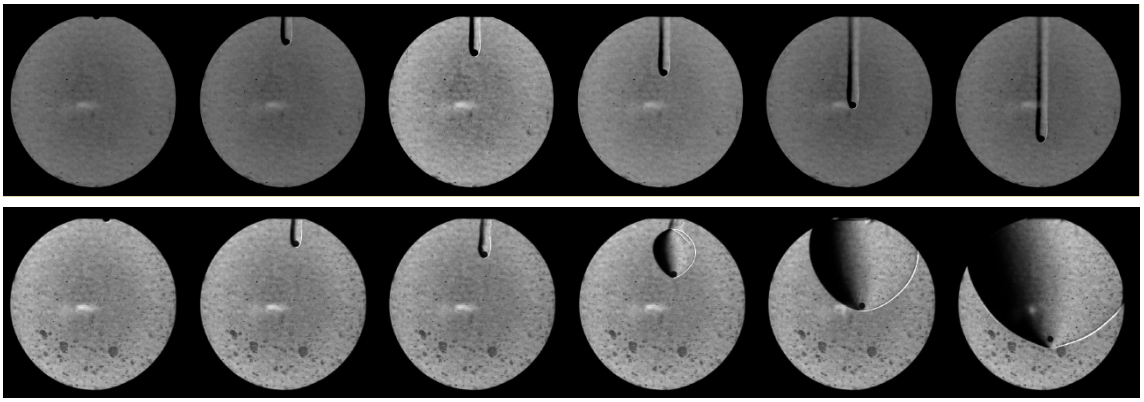

1.2 ms 10.0 ms 13.6 ms 20.0 ms 30.0 ms 40.0 ms

Figure 2: Schlieren images of a no ignition case for T_{sphere}=1083 K (top) and an ignition case for T_{sphere}=1153 K (bottom). Conditions: *n*-hexane-air at Φ=0.9; P_1=100 kPa; T_1=300 K.

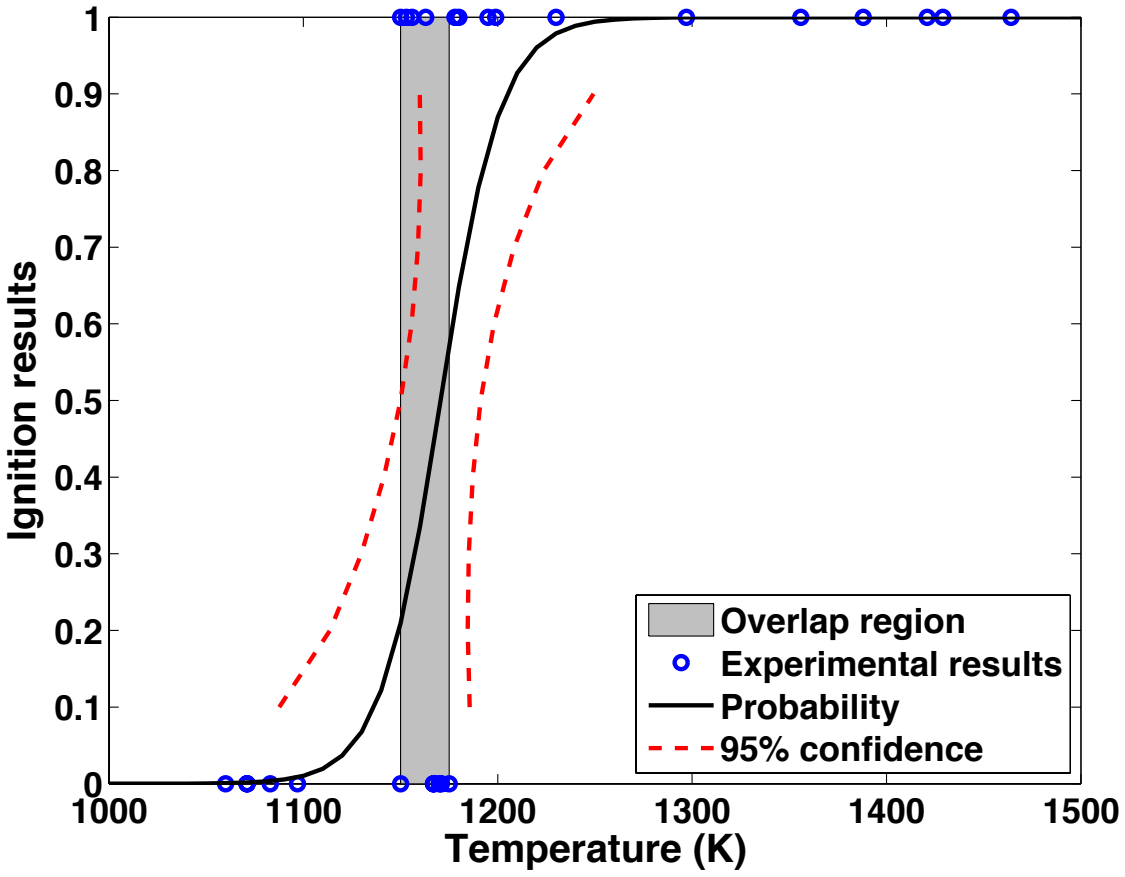

Figure 3: Ignition results for 4 mm diameter sphere with a speed of 2.4 m/s. Conditions: *n*-hexane-air at Φ=0.9; P_1=100 kPa; T_1=300 K.

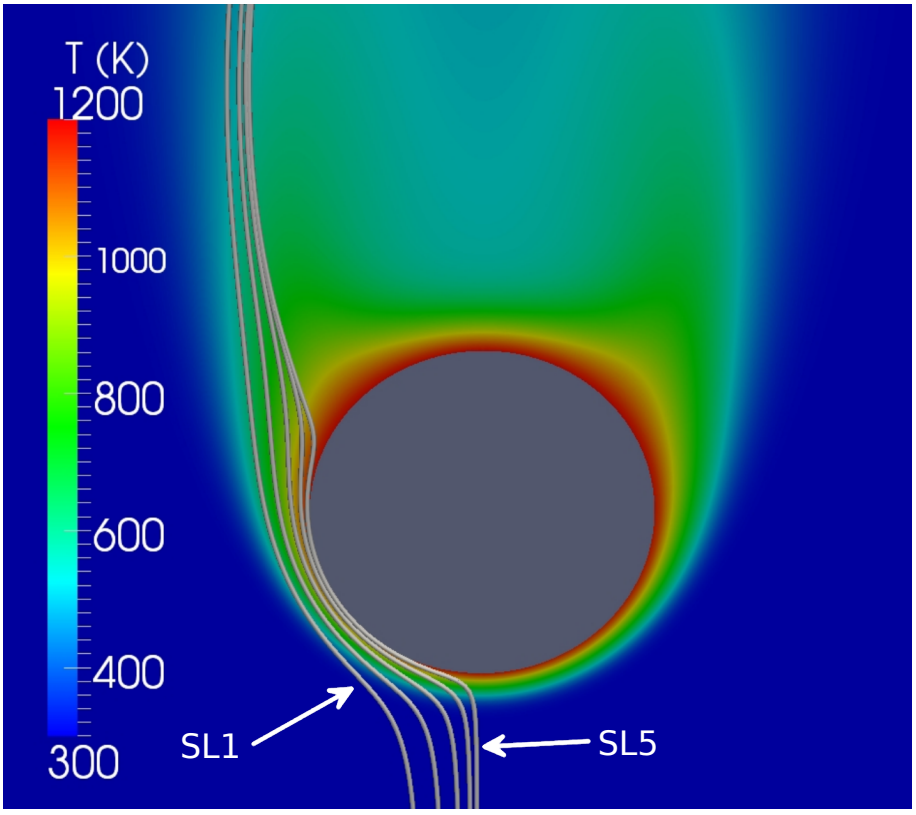

a) Streamlines

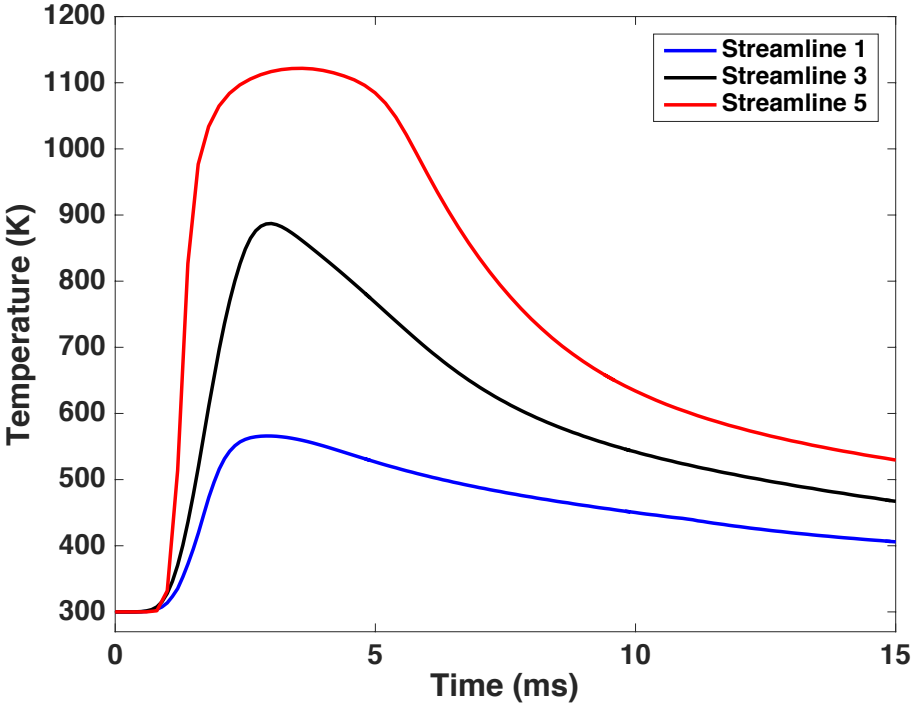

b) Temperature profiles

Figure 4: Results from 2D non-reactive simulation of a hot sphere falling in N_2. a): temperature field and streamline positions. b): temperature histories of three fluid parcels traveling along streamlines. Conditions: X_{N2}=1; P_1=100 kPa; T_1=300 K; T_{sphere}=1200 K; U_1=0 m/s.

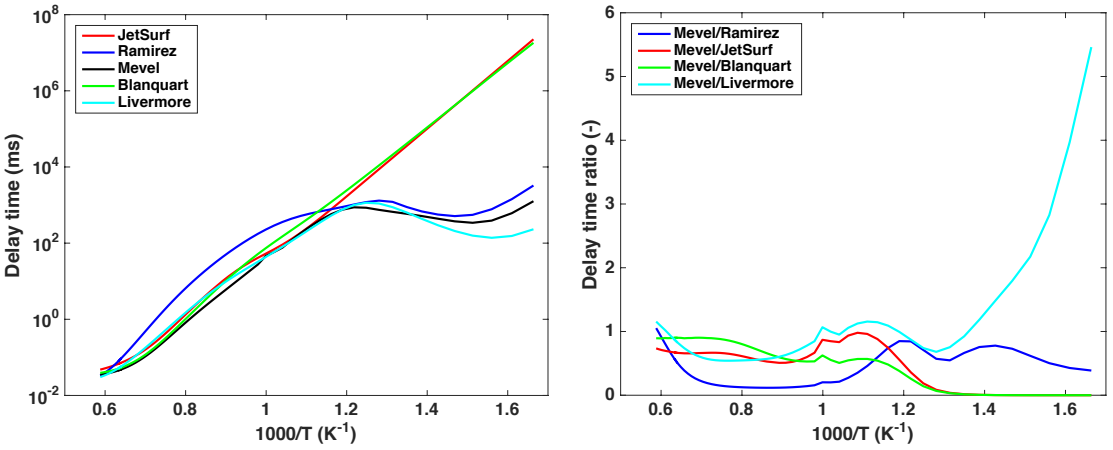

a) Delay times b) Delay time ratios

Figure 5: a) Comparison between the predicted ignition delay time of a *n*-hexane-air mixture by several detailed reaction models. b) Ratios of the predicted delay times by several detailed reaction models. Conditions: Φ=0.9; P_1=100 kPa.

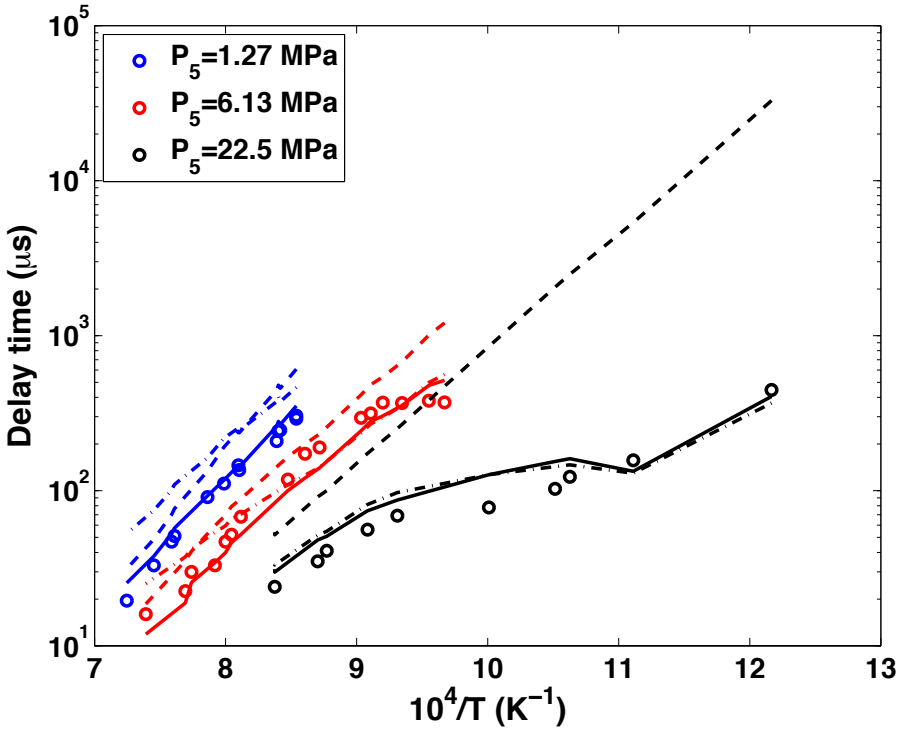

a) Zhukov et al. (2004)

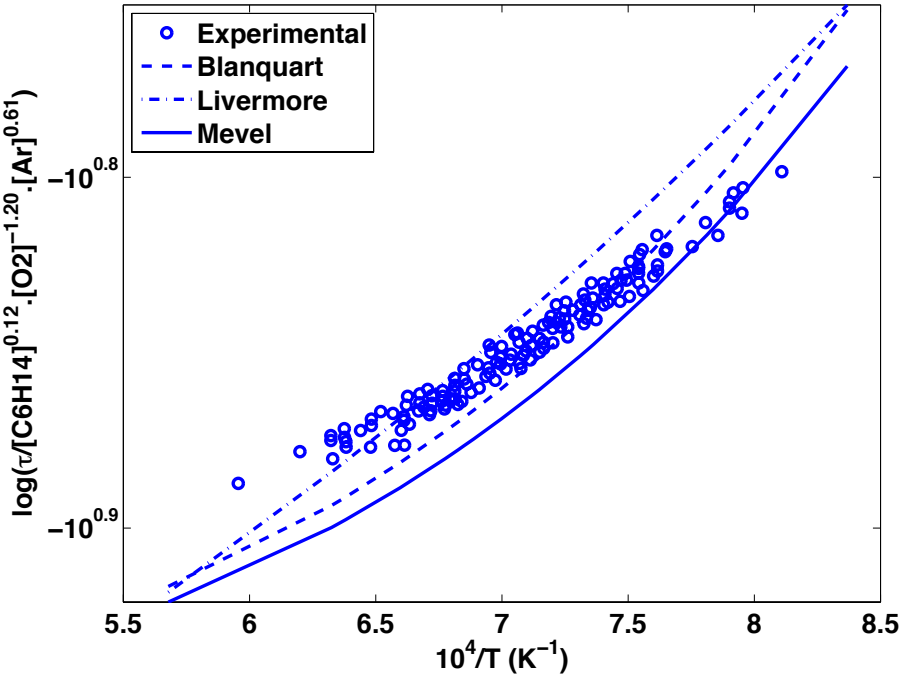

b) Burcat el al. (1996)

Figure 6: Comparison between the experimental ignition delay time for n-hexane and the prediction of several reaction models. Experimental conditions: a): Φ=0.5, X_{Ar}=0.7812; P_5=1.14-6.69 MPa; Solid lines: Mével; Dashed Lines: Blanquart; Dashed-dotted lines: Livermore. b): Φ=0.5-2, X_{Ar}=0.79-0.9475, P_5=300-844 kPa.

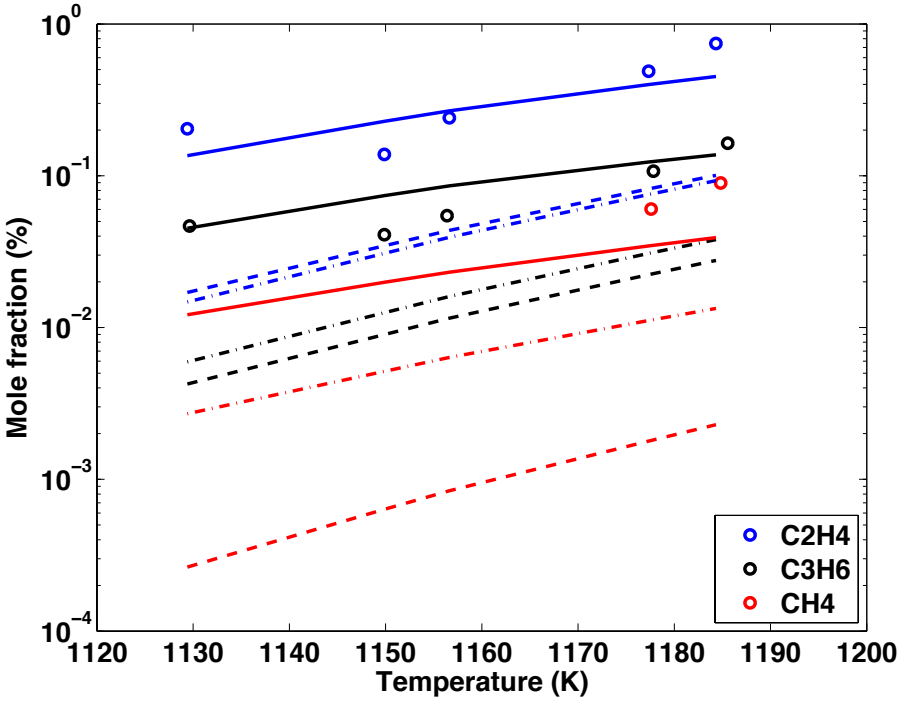

Figure 7: Comparison between the experimental species profiles obtained during the oxidation of n-hexane, Burcat el al. (1996), and the prediction of several reaction models. Experimental conditions: Φ=1, X_{Ar}=0.895; P_5=300 kPa (estimated); T_5=1130-1185 K; Residence time=250 μs. Solid lines: Mével; Dashed Lines: Blanquart; Dashed-dotted lines: Livermore.

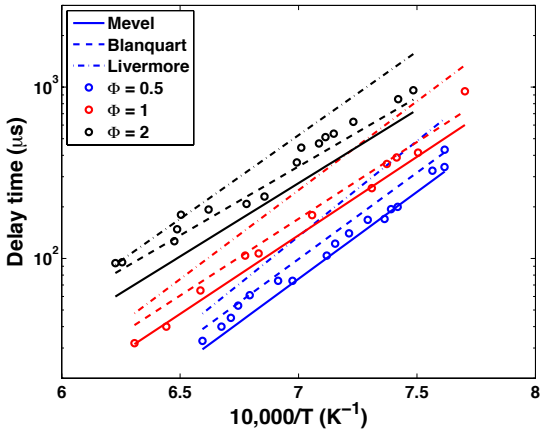

a) Present study

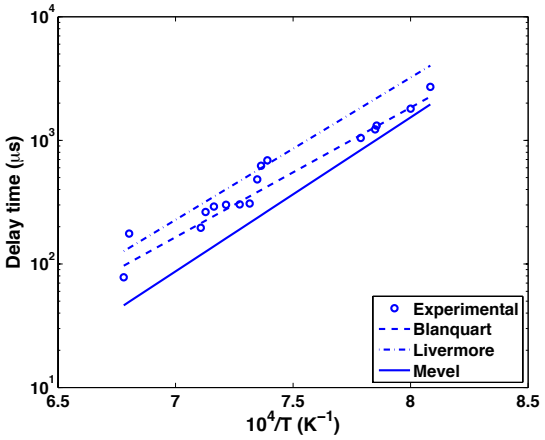

b) Davidson et al., 2010

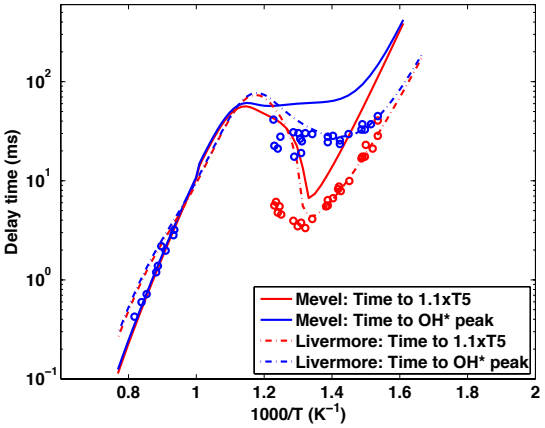

c) Campbell et al., 2015

Figure 8: Comparison between the experimental ignition delay time for n-hexane a) and b) and n-heptane c) and the prediction of the several reaction models. Experimental conditions: a): Φ=0.5-2, X_{Ar}=0.96; P_5=350 kPa; b): Φ=1, X_{Ar}=0.9558, P_5=178-365 kPa; c): Φ=0.75, X_{CO2}=0.0500, X_{Ar}=0.7898, P_5=659 kPa. In simulations for Campbell et al. (2015) data, n-hexane is used instead of n-heptane.

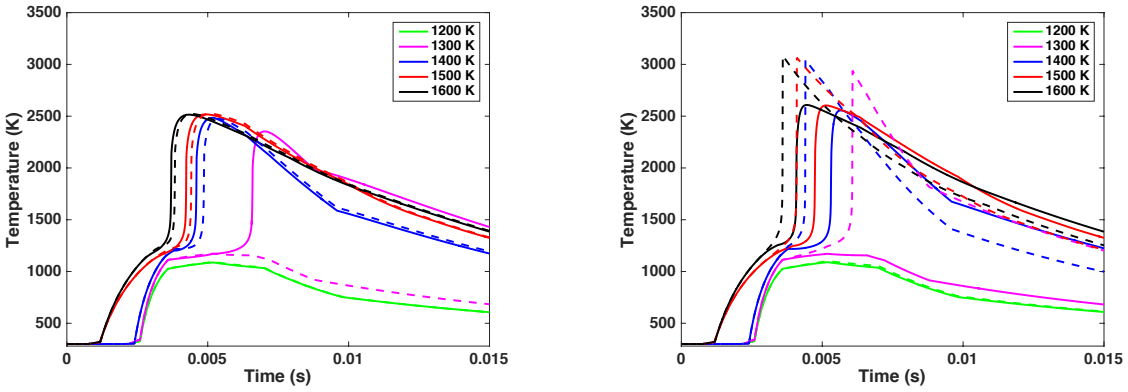

a): Mével (solid) and Blanquart (dashed) b): Livermore (solid) and one-step (dashed)

Figure 9: Comparison between the estimated gas temperature histories using the model of Equation 8 and Equation 9 along the streamline closest to the sphere for different surface temperatures obtained with several reaction models. Conditions: n-hexane-air at Φ=0.9; P_1=100 kPa; T_{sphere}=1200-1600 K.

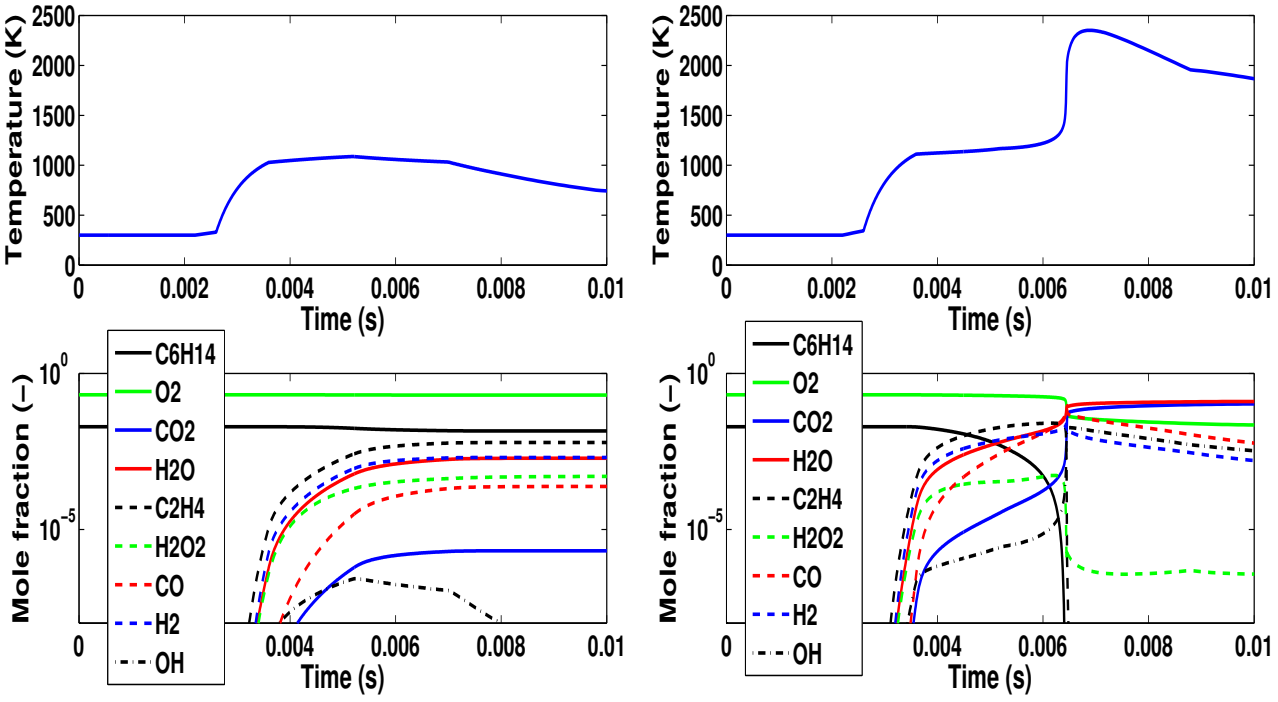

a) T_s=1200 K b) T_s=1300 K

Figure 10: Gas temperature and species profiles computed using the model of Equation 8 and Equation 9 along the streamline closest to the sphere for different surface temperatures obtained with Mével's detailed chemical model. Conditions: *n*-hexane-air at Φ=0.9; P_1=100 kPa.

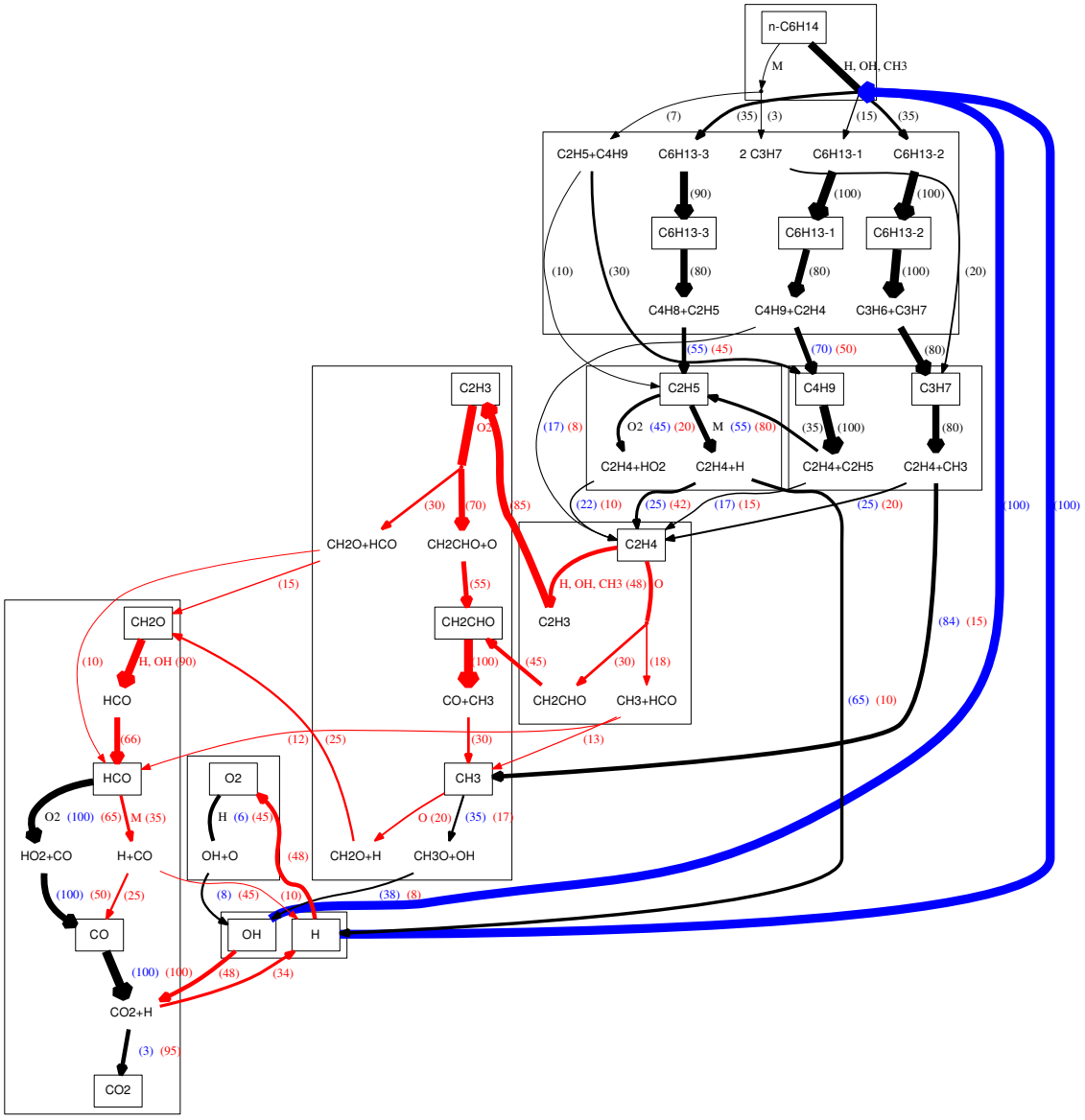

Figure 11: Reaction pathways computed using the model of Equation 8 and Equation 9 along the streamline closest to the sphere for different surface temperatures obtained with Mével's detailed chemical model. Conditions:n-hexane-air at Φ=0.9; P_1=100 kPa. Common paths: black. Specific paths: blue for T_s=1200 K and red for T_s=1300 K.